



POLITECNICO
DI TORINO
Department of MEchanical
and AeroSpace Engineering



HR EXCELLENCE IN RESEARCH



Advanced FEs for the micropolar and geometrical nonlinear analyses of composite structures

Riccardo Augello
Turin, 28th October 2020

Supervisors: Prof. E. Carrera, Prof. A. Pagani, Prof. C.W. Lim



香港城市大學
City University of Hong Kong



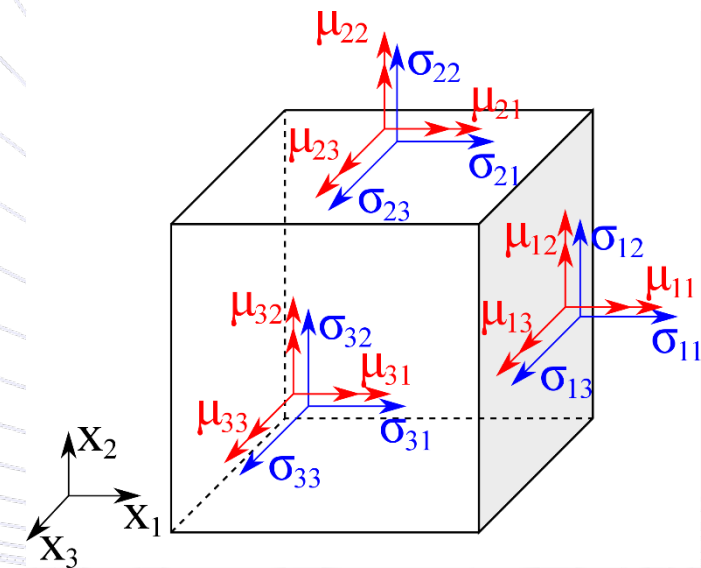
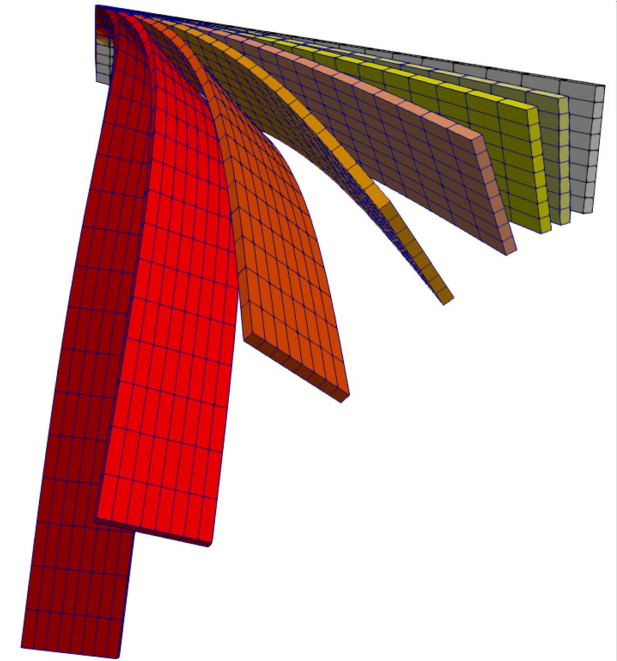
Compagnia
di San Paolo

- Introduction
- 1D and 2D plate/shell unified model
- Geometrical nonlinear formulation
 - Nonlinear geometrical relation and constitutive equation
 - Numerical results – static analysis
 - Modal properties
 - Numerical results – modal analysis
- Micropolar Elasticity
 - Motivation
 - Formulation
 - Numerical results
- Conclusions

Introduction



The elastic, geometrical nonlinear analysis of structures has always been a fundamental topic in structural mechanics. It is a matter of fact that the effects of large displacements and rotations may play a primary role in the correct prediction, for example, of wing structures, space antennas, robotic arms, as well as turbine blades, among others. Then, the availability of accurate models able to deal with postbuckling and large displacement analysis is of crucial relevance.

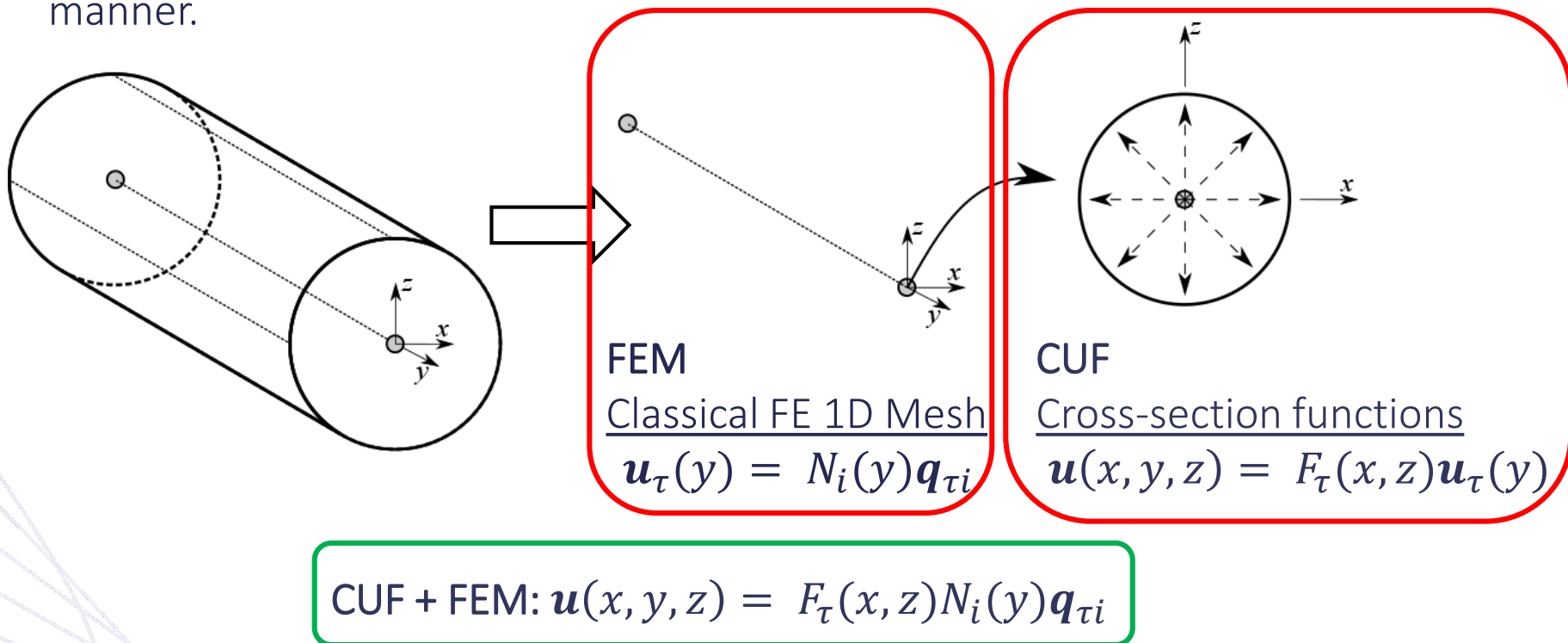


In many cases, Classical Elasticity (CE) may fail on accurately describing the behavior of structures. Besides, when the size of the analyzed structure is comparable to the microstructural scale, the body behaves quite differently from the prediction that CE could lead to. For this reason, several generalized continua models have been developed. Among the generalized continuum theories, Micropolar Elasticity (ME) deserves particular attention.

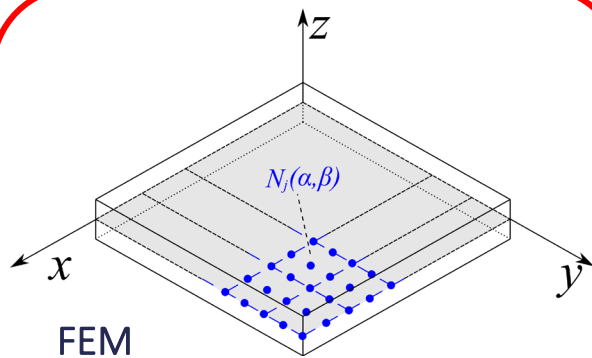
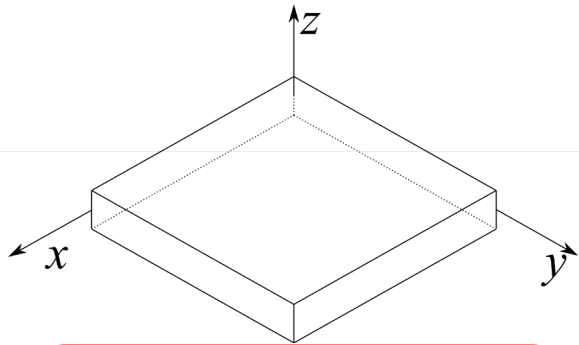
1D beam unified model



- The Carrera Unified Formulation (CUF) is a hierarchical formulation, according to which the order of the theory can be set as an input of the analysis. Any order beam theories can be implemented in an automatic manner.



2D plate/shell unified model



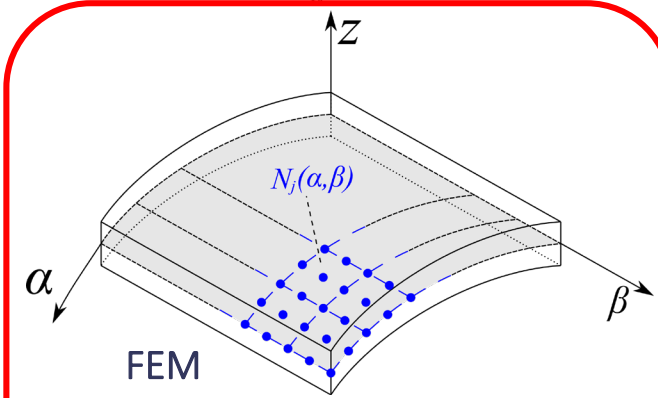
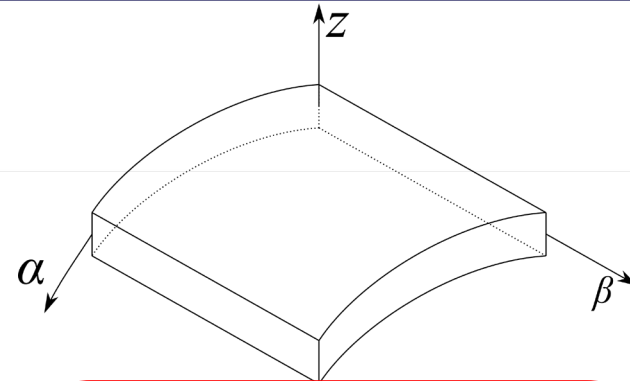
FEM

Classical FE 2D Mesh

$$\mathbf{u}_\tau(x, y) = \mathbf{N}_i(x, y)\mathbf{q}_{\tau i}$$

CUF + FEM:

$$\mathbf{u}(x, y, z) = F_\tau(z)\mathbf{N}_i(x, y)\mathbf{q}_{\tau i}$$



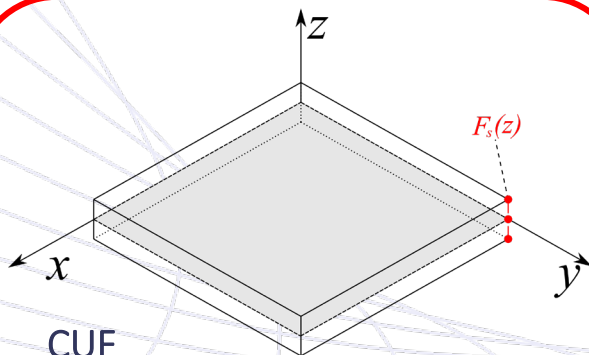
FEM

Classical FE 2D Mesh

$$\mathbf{u}_\tau(\alpha, \beta) = \mathbf{N}_i(\alpha, \beta)\mathbf{q}_{\tau i}$$

CUF + FEM:

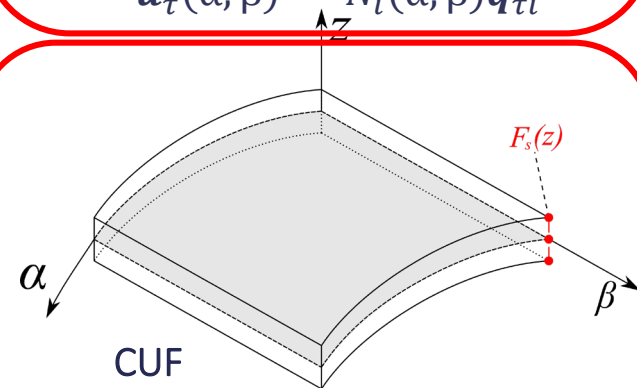
$$\mathbf{u}(x, y, z) = F_\tau(z)\mathbf{N}_i(\alpha, \beta)\mathbf{q}_{\tau i}$$



CUF

Cross-section functions

$$\mathbf{u}(\alpha, \beta, z) = F_\tau(z)\mathbf{u}_\tau(\alpha, \beta)$$



CUF

Cross-section functions

$$\mathbf{u}(x, y, z) = F_\tau(z)\mathbf{u}_\tau(x, y)$$

Geometric nonlinear formulation

- Nonlinear geometrical relation and constitutive equation (1)



$$\begin{Bmatrix} \epsilon_{yy} \\ \epsilon_{xx} \\ \epsilon_{zz} \\ \epsilon_{xz} \\ \epsilon_{yz} \\ \epsilon_{xy} \end{Bmatrix} = (\mathbf{b}_l + \mathbf{b}_{nl}) \begin{Bmatrix} u_x \\ u_y \\ u_z \end{Bmatrix}$$

Green-Lagrange strains

1D BEAM &
2D PLATE

$$\mathbf{b}_l = \begin{bmatrix} \partial_x & 0 & 0 \\ 0 & \partial_y & 0 \\ 0 & 0 & \partial_z \\ \partial_z & 0 & \partial_x \\ 0 & \partial_z & \partial_y \\ \partial_y & \partial_x & 0 \end{bmatrix}$$

$$\mathbf{b}_{nl} = \begin{bmatrix} \frac{1}{2} (\partial_x)^2 & \frac{1}{2} (\partial_x)^2 & \frac{1}{2} (\partial_x)^2 \\ \frac{1}{2} (\partial_y)^2 & \frac{1}{2} (\partial_y)^2 & \frac{1}{2} (\partial_y)^2 \\ \frac{1}{2} (\partial_z)^2 & \frac{1}{2} (\partial_z)^2 & \frac{1}{2} (\partial_z)^2 \\ \partial_x \partial_z & \partial_x \partial_z & \partial_x \partial_z \\ \partial_y \partial_z & \partial_y \partial_z & \partial_y \partial_z \\ \partial_x \partial_y & \partial_x \partial_y & \partial_x \partial_y \end{bmatrix}$$

2D SHELL

$$\mathbf{b}_l = \begin{bmatrix} \frac{\partial_z}{H_x} & 0 & \frac{1}{H_x R_x} \\ 0 & \frac{\partial_\beta}{H_\beta} & \frac{1}{H_\beta R_\beta} \\ 0 & 0 & \partial_z \\ \partial_z - \frac{1}{H_x R_x} & 0 & \frac{\partial_z}{H_x} \\ 0 & \partial_z - \frac{1}{H_\beta R_\beta} & \frac{\partial_\beta}{H_\beta} \\ \frac{\partial_\beta}{H_\beta} & \frac{\partial_z}{H_x} & 0 \end{bmatrix}$$

$$\mathbf{b}_{nl} = \begin{bmatrix} \frac{1}{2H_x^2} \left[(\partial_x)^2 + \frac{2u_z \partial_z}{R_x} + \frac{u_x}{R_x^2} \right] & \frac{(\partial_x)^2}{2H_x^2} & \frac{1}{2H_x^2} \left[(\partial_x)^2 - \frac{2u_x \partial_x}{R_x} + \frac{u_z}{R_x^2} \right] \\ \frac{(\partial_\beta)^2}{2H_\beta^2} & \frac{1}{2H_\beta^2} \left[(\partial_\beta)^2 + \frac{2u_z \partial_\beta}{R_\beta} + \frac{u_\beta}{R_\beta^2} \right] & \frac{1}{2H_\beta^2} \left[(\partial_\beta)^2 - \frac{2u_\beta \partial_\beta}{R_\beta} + \frac{u_z}{R_\beta^2} \right] \\ \frac{1}{2} (\partial_z)^2 & \frac{1}{2} (\partial_z)^2 & \frac{1}{2} (\partial_z)^2 \\ \frac{1}{H_x} \left(\partial_x \partial_z + \frac{u_z \partial_z}{R_x} \right) & \frac{\partial_x \partial_z}{H_x} & \frac{1}{H_x} \left(\partial_x \partial_z - \frac{u_x \partial_z}{R_x} \right) \\ \frac{\partial_\beta \partial_z}{H_\beta} & \frac{1}{H_\beta} \left(\partial_\beta \partial_z + \frac{u_z \partial_z}{R_\beta} \right) & \frac{1}{H_\beta} \left(\partial_\beta \partial_z - \frac{u_\beta \partial_z}{R_\beta} \right) \\ \frac{1}{H_x H_\beta} \left(\partial_x \partial_\beta + \frac{u_z \partial_\beta}{R_x} + \frac{u_\beta}{R_x R_\beta} \right) & \frac{1}{H_x H_\beta} \left(\partial_x \partial_\beta + \frac{u_z \partial_x}{R_\beta} \right) & \frac{1}{H_x H_\beta} \left(\partial_x \partial_\beta - \frac{u_x \partial_\beta}{R_x} - \frac{u_\beta \partial_x}{R_\beta} \right) \end{bmatrix}$$

Geometric nonlinear formulation

- Nonlinear geometrical relation and constitutive equation (2)



$$\begin{Bmatrix} \epsilon_{yy} \\ \epsilon_{xx} \\ \epsilon_{zz} \\ \epsilon_{xz} \\ \epsilon_{yz} \\ \epsilon_{xy} \end{Bmatrix} = (\mathbf{b}_l + \mathbf{b}_{nl}) \begin{Bmatrix} u_x \\ u_y \\ u_z \end{Bmatrix} = (\mathbf{B}_l + \mathbf{B}_{nl}) \begin{Bmatrix} q_{x\tau i} \\ q_{y\tau i} \\ q_{z\tau i} \end{Bmatrix}, \text{ Where: } \begin{cases} \mathbf{B}_l = \mathbf{b}_l(F_\tau N_i) \\ \mathbf{B}_{nl} = \begin{bmatrix} \frac{1}{2} u_{x,y} F_\tau N_{i,y} & \dots \\ \frac{1}{2} u_{x,x} F_{\tau,x} N_i & \dots \\ \vdots & \vdots \\ \frac{1}{2} u_{x,x} F_{\tau,z} N_i + \frac{1}{2} u_{x,z} F_{\tau,x} N_i & \dots \\ \vdots & \vdots \end{bmatrix} \end{cases}$$

$$\boldsymbol{\sigma} = \mathbf{C}\boldsymbol{\epsilon} = \mathbf{C}(\mathbf{B}_l + \mathbf{B}_{nl}) \begin{Bmatrix} q_{x\tau i} \\ q_{y\tau i} \\ q_{z\tau i} \end{Bmatrix}$$

Constitutive relation

$$\mathbf{C} = \begin{bmatrix} C_{11} & C_{12} & C_{13} & 0 & 0 & 0 \\ C_{12} & C_{22} & C_{23} & 0 & 0 & 0 \\ C_{13} & C_{23} & C_{33} & 0 & 0 & 0 \\ 0 & 0 & 0 & C_{44} & 0 & 0 \\ 0 & 0 & 0 & 0 & C_{55} & 0 \\ 0 & 0 & 0 & 0 & 0 & C_{66} \end{bmatrix}$$

$$\tilde{\mathbf{C}} = \begin{bmatrix} \tilde{C}_{11} & \tilde{C}_{12} & \tilde{C}_{13} & 0 & 0 & \tilde{C}_{16} \\ & \tilde{C}_{22} & \tilde{C}_{23} & 0 & 0 & \tilde{C}_{26} \\ & & \tilde{C}_{33} & 0 & 0 & \tilde{C}_{36} \\ & & & \tilde{C}_{44} & \tilde{C}_{45} & 0 \\ & & & & \tilde{C}_{55} & 0 \\ \text{sym.} & & & & & \tilde{C}_{66} \end{bmatrix}$$

Geometric nonlinear formulation

- Principle of virtual work



$$\delta L_{\text{int}} = \delta L_{\text{ext}}$$

"Secant" stiffness matrix:

$$\begin{aligned} \delta L_{\text{int}} &= \delta \mathbf{q}_{sj}^T \left\langle \left(\mathbf{B}_l^{sj} + 2\mathbf{B}_{nl}^{sj} \right)^T \mathbf{C} \left(\mathbf{B}_l^{\tau i} + \mathbf{B}_{nl}^{\tau i} \right) \right\rangle \mathbf{q}_{\tau i} \\ &= \delta \mathbf{q}_{sj}^T \mathbf{K}_{0}^{ij\tau s} \mathbf{q}_{\tau i} + \delta \mathbf{q}_{sj}^T \mathbf{K}_{lnl}^{ij\tau s} \mathbf{q}_{\tau i} + \delta \mathbf{q}_{sj}^T \mathbf{K}_{nll}^{ij\tau s} \mathbf{q}_{\tau i} + \delta \mathbf{q}_{sj}^T \mathbf{K}_{nl nl}^{ij\tau s} \mathbf{q}_{\tau i} \\ &= \delta \mathbf{q}_{sj}^T \mathbf{K}_S^{ij\tau s} \mathbf{q}_{\tau i} \end{aligned}$$



A. Pagani, E. Carrera, "Unified formulation of geometrically nonlinear refined beam theories", Mechanics of Advanced Materials and Structures, 2017.

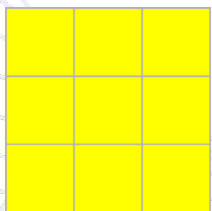


E. Carrera, A. Pagani, R. Augello, "On the role of large cross-sectional deformations in the nonlinear analysis of composite thin-walled structures", Archive of Applied Mechanics, 2021.

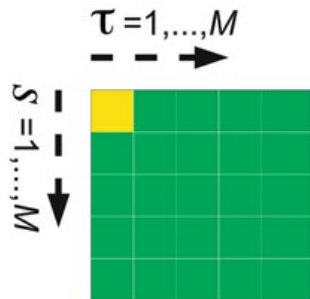
$$\delta L_{\text{ext}} = F_s(x_p, z_p) N_j(y_p) \delta \mathbf{q}_{sj}^T \mathbf{P} = \delta \mathbf{q}_{sj}^T \mathbf{p}_{sj}$$

$$\mathbf{K}_S^{ij\tau s} \mathbf{q}_{\tau i} - \mathbf{p}_{sj} = 0$$

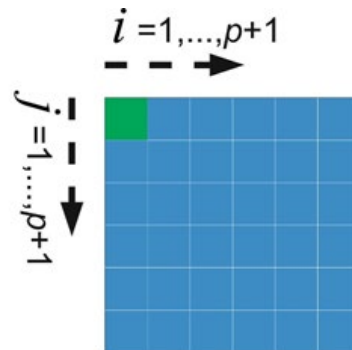
$$\mathbf{K}_S \mathbf{q} - \mathbf{p} = 0$$



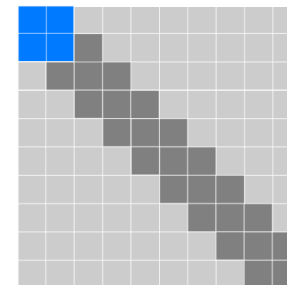
3x3 NUCLEUS



NODE



ELEMENT



STRUCTURE



Geometric nonlinear formulation

- Newton-Raphson linearization with arc-length constraint



$$\boldsymbol{\varphi}_{res} \equiv \mathbf{K}_S \mathbf{q} - \mathbf{p} = 0$$

$$\boldsymbol{\varphi}_{res}(\mathbf{q} + \delta \mathbf{q}, \mathbf{p} + \delta \mathbf{p}) = \boldsymbol{\varphi}_{res}(\mathbf{q}, \mathbf{p}) + \frac{\partial \boldsymbol{\varphi}_{res}}{\partial \mathbf{q}} \delta \mathbf{q} + \frac{\partial \boldsymbol{\varphi}_{res}}{\partial \mathbf{p}} \delta \lambda \mathbf{p}_{ref} = 0$$

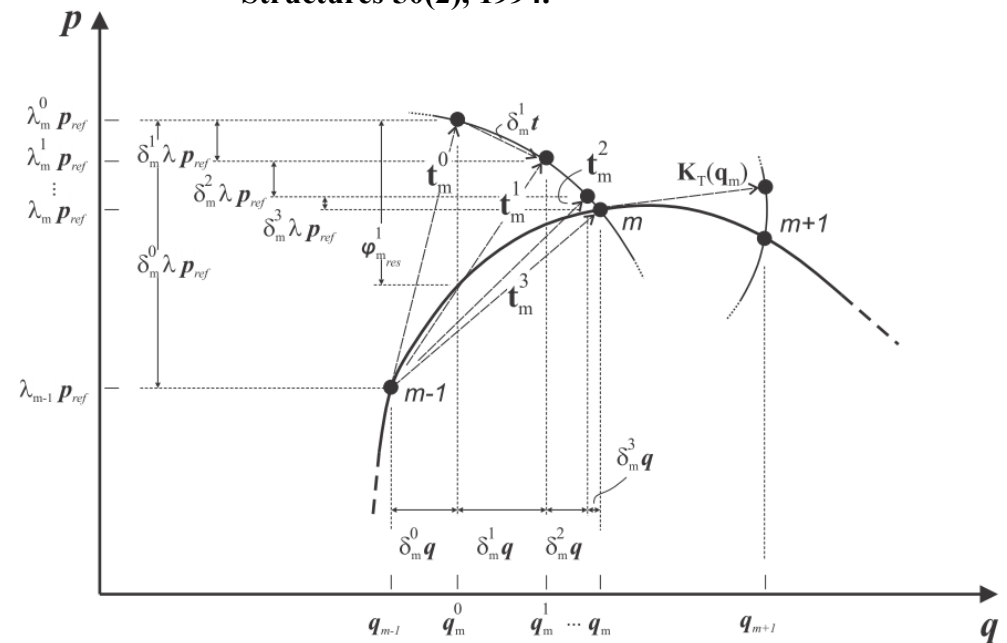
“Tangent” stiffness matrix:

$$\begin{aligned} \delta(\delta L_{int}) &= \langle \delta(\delta \boldsymbol{\epsilon}^T \boldsymbol{\sigma}) \rangle \\ &= \langle \delta \boldsymbol{\epsilon}^T \delta \boldsymbol{\sigma} \rangle + \langle \delta(\delta \boldsymbol{\epsilon}^T) \boldsymbol{\sigma} \rangle \\ &= \delta \mathbf{q}_{sj}^T (\mathbf{K}_0^{ij\tau s} + \mathbf{K}_{T_1}^{ij\tau s} + \mathbf{K}_{\sigma}^{ij\tau s}) \delta \mathbf{q}_{\tau i} \\ &= \delta \mathbf{q}_{sj}^T \mathbf{K}_T^{ij\tau s} \delta \mathbf{q}_{\tau i} \end{aligned}$$

$$\begin{cases} \mathbf{K}_T \delta \mathbf{q} = \delta \lambda \mathbf{p}_{ref} - \boldsymbol{\varphi}_{res} \\ c(\delta \mathbf{q}, \delta \lambda) = 0 \end{cases}$$



E. Carrera, “A study on arc-length-type methods and their operation failures illustrated by a simple model”, Computers and Structures 50(2), 1994.

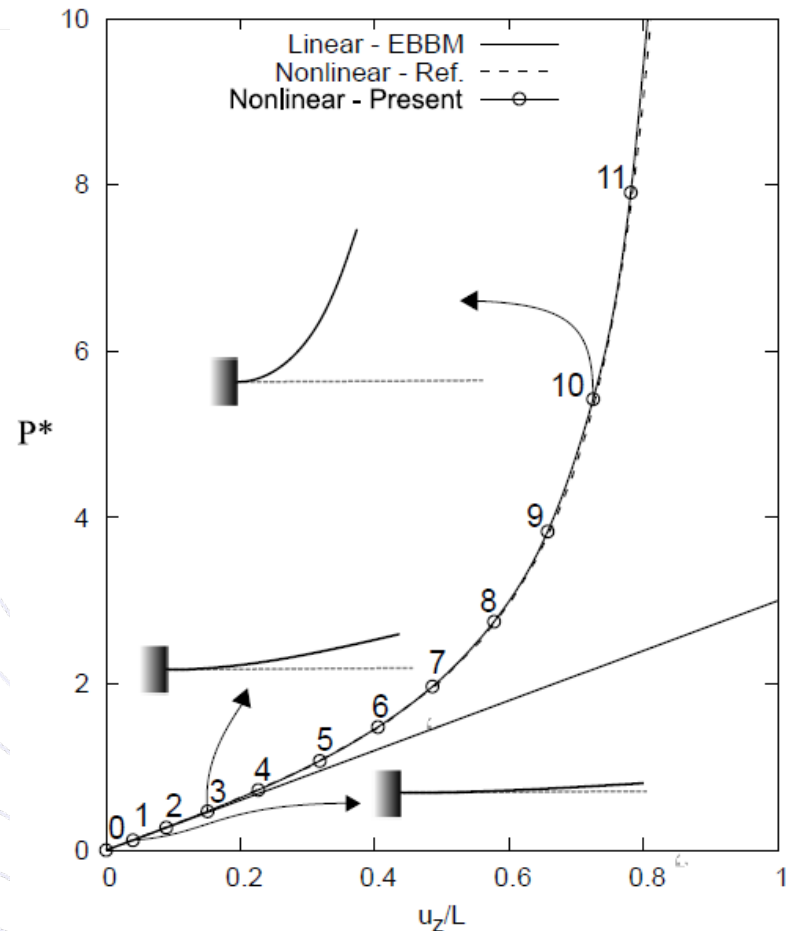


Numerical results – static analysis - 1D model

- Large deflection and post-buckling of cantilever isotropic beam

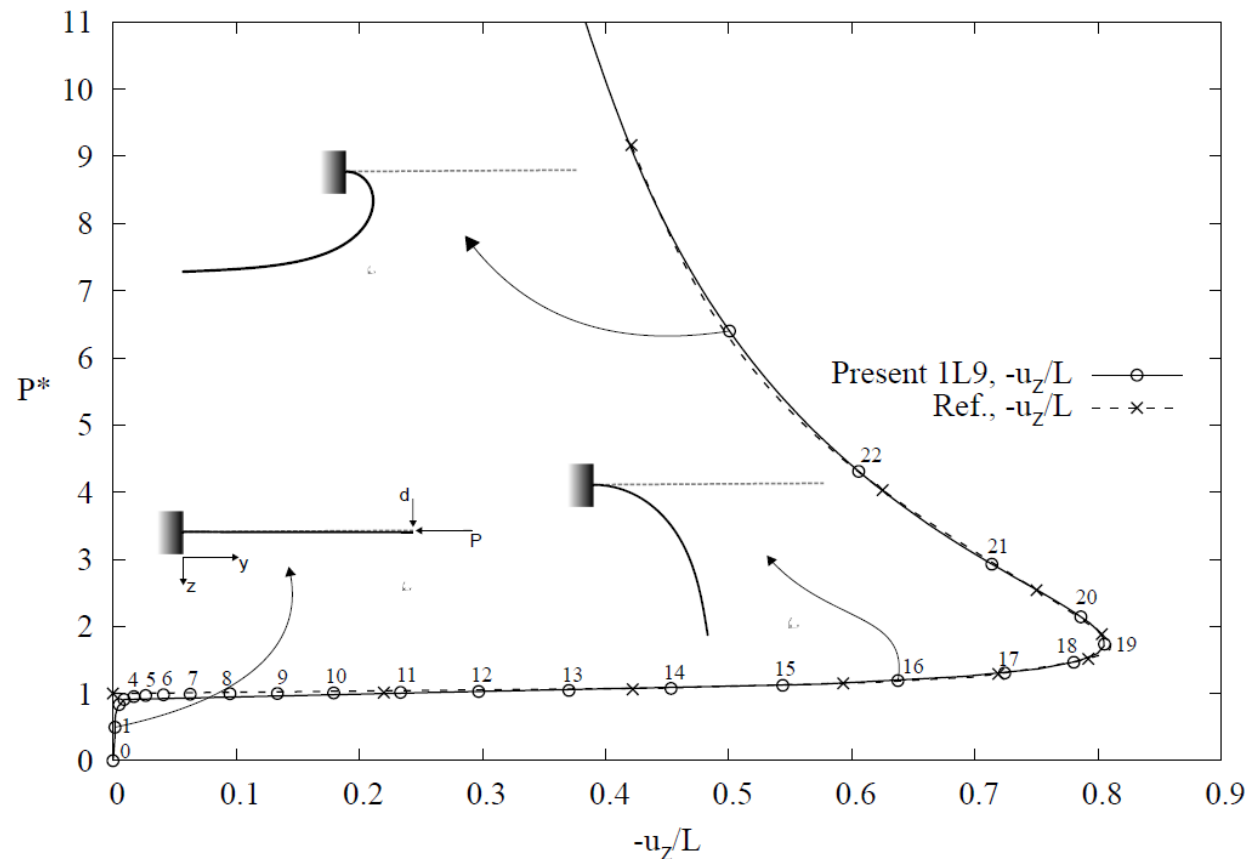


Large deflection



(b) $\frac{L}{h} = 100$

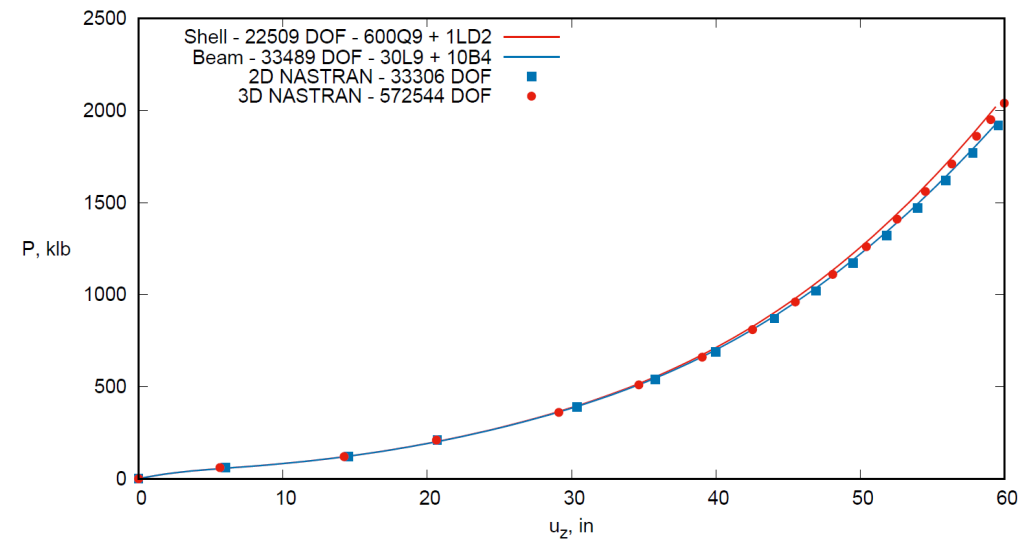
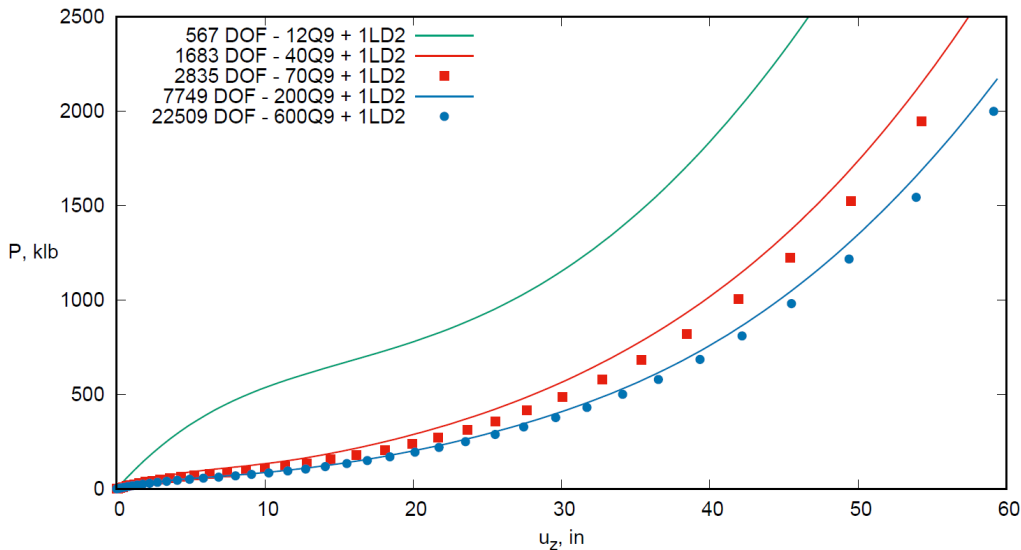
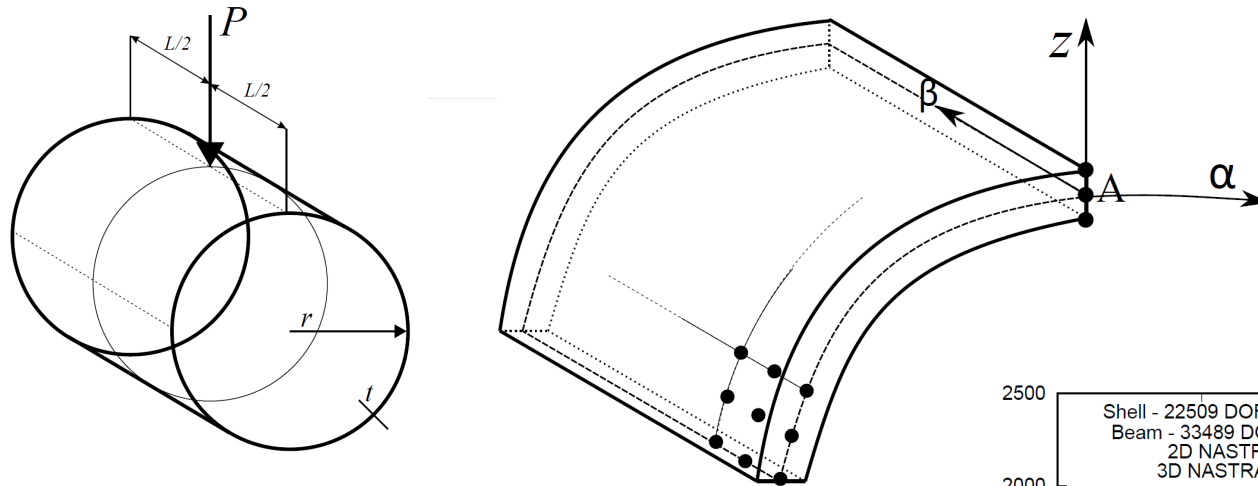
Post-buckling



A. Pagani , R. Augello, E. Carrera,
“Frequency and mode change in the large
deflection and post-buckling of compact and
thin-walled beams”, Journal of Sound and
Vibration, 2018.

Numerical results – static analysis - 2D shell model

- Pinched isotropic cylinder



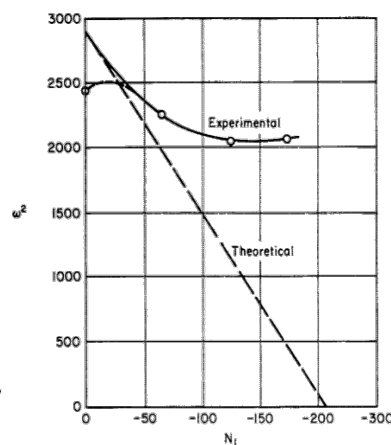
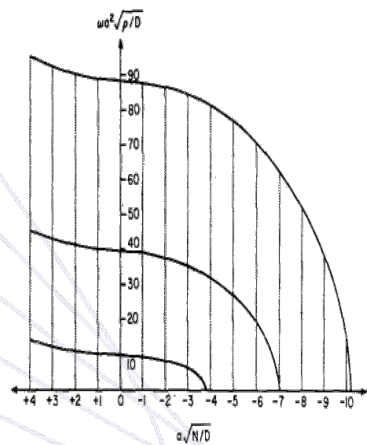
E. Carrera, A. Pagani, R. Augello, B. Wu, "Popular benchmarks of nonlinear shell analysis solved by 1D and 2D CUF-based finite elements", Mechanics of Advanced Materials and Structures, 2020.

VCT - Mode aberration



The influence of initial stress on both the static and dynamic response of elastic bodies has been studied extensively by a variety of investigators by pertinent **linearization** of the nonlinear equations of elasticity.

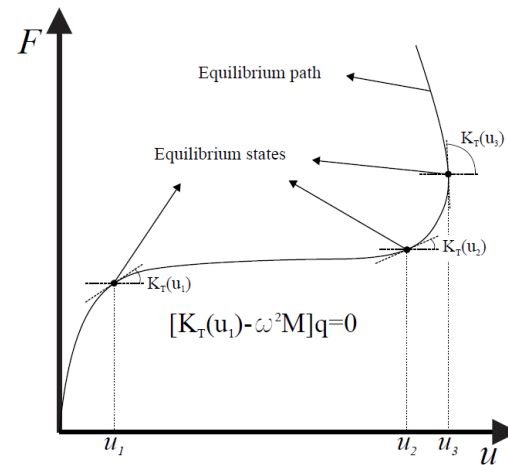
Because the modal behavior of structures are evidently a property of the equilibrium state, dynamic response is subjected to changes.



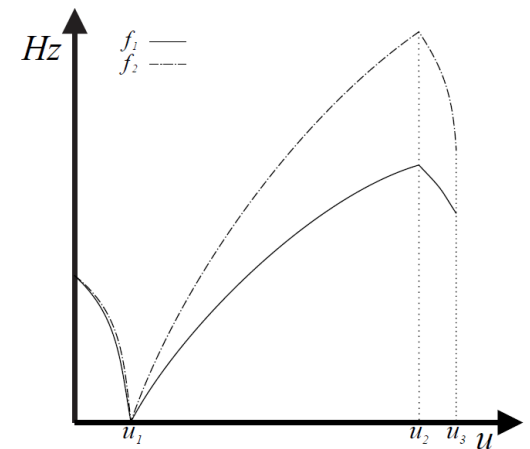
A.W. Leissa,
“*Vibration of plates*”,
NASA Tech. Rept.,
1969.



H. Lurie, ““*Lateral Vibrations as Related to Structural Stability*”, J. App. Mech., 1952.



(a) Eigenvalue problem at equilibrium states



(b) Natural frequencies trend

Geometric nonlinear formulation

- Dynamic analysis



The evaluation of the linearized free vibration modes around nonlinear equilibrium states:

$$\delta(\delta L_{\text{int}}) = -\delta(\delta L_{\text{ine}})$$

$$\delta(\delta L_{\text{ine}}) = \delta \left(\int_V \delta \mathbf{u}^T \boldsymbol{\rho} \ddot{\mathbf{u}} dV \right) = \delta \left(\delta \mathbf{q}_{sj}^T \mathbf{M}^{ij\tau s} \ddot{\mathbf{q}}_{\tau i} \right)$$

$$= \delta \mathbf{q}_{sj}^T \mathbf{M}^{ij\tau s} \delta \ddot{\mathbf{q}}_{\tau i}$$

$$\delta \mathbf{q}_{\tau i}^T \mathbf{K}_T^{ij\tau s} \delta \mathbf{q}_{sj} = -\delta \mathbf{q}_{\tau i}^T \mathbf{M}^{ij\tau s} \delta \ddot{\mathbf{q}}_{sj}$$

Given the nature of the problem in hand and the hypothesis made, it is reasonable to assume harmonic motion around linearized states along the nonlinear equilibrium path. Thus, one has:

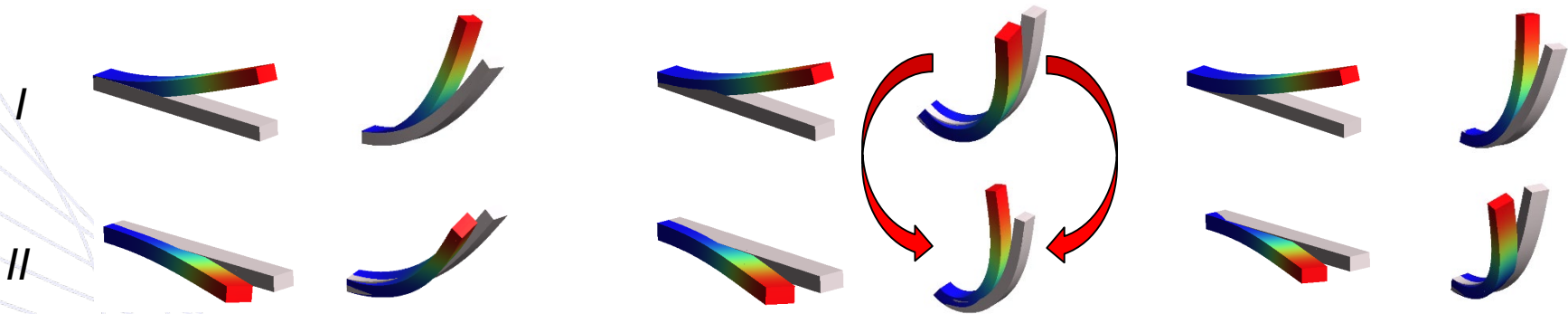
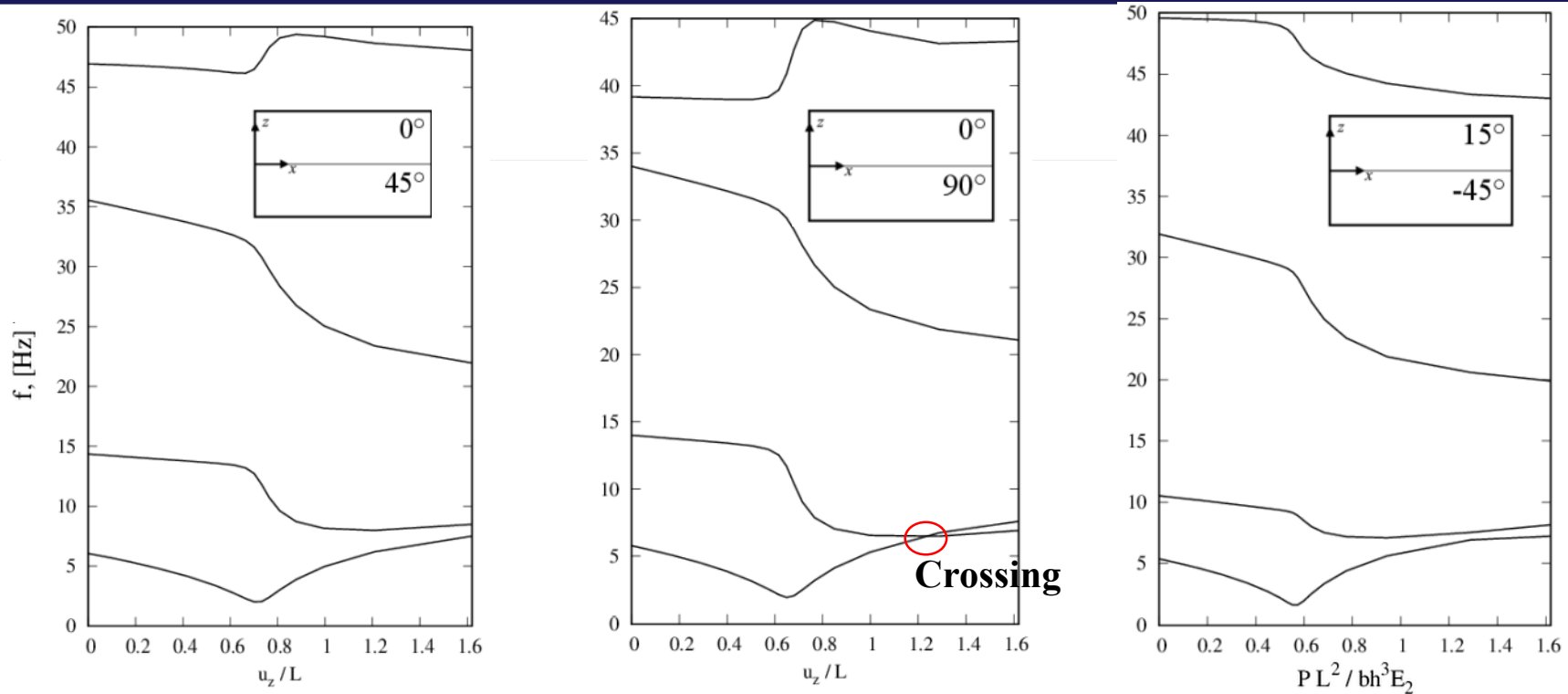
$$\delta \mathbf{q}_{sj}(t) = \delta \bar{\mathbf{q}}_{sj} e^{i\omega t}$$

$$\delta \ddot{\mathbf{q}}_{\tau i}(t) = -\omega^2 \delta \bar{\mathbf{q}}_{sj} e^{i\omega t}$$

$$\left(\mathbf{K}_T^{ij\tau s} - \omega^2 \mathbf{M}^{ij\tau s} \right) \delta \bar{\mathbf{q}}_{sj} = 0$$

Numerical results – modal analysis - 1D model

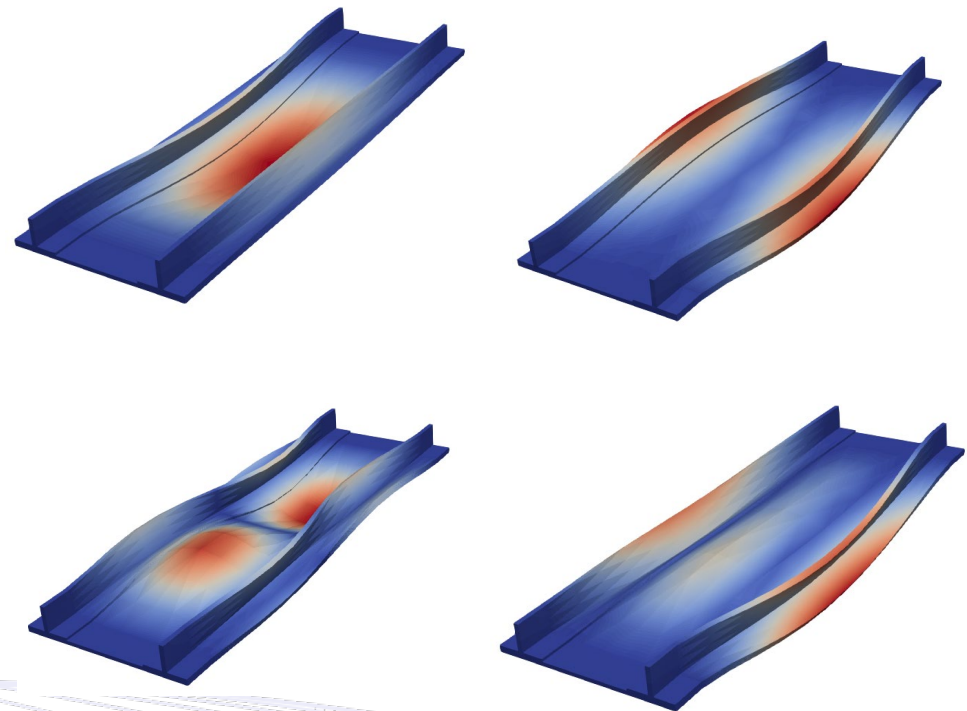
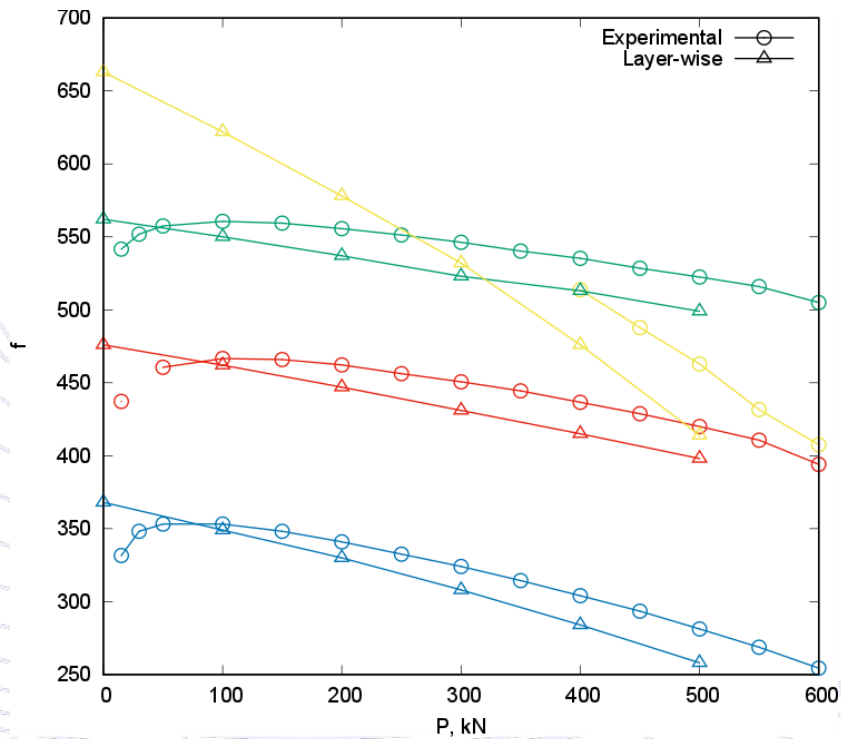
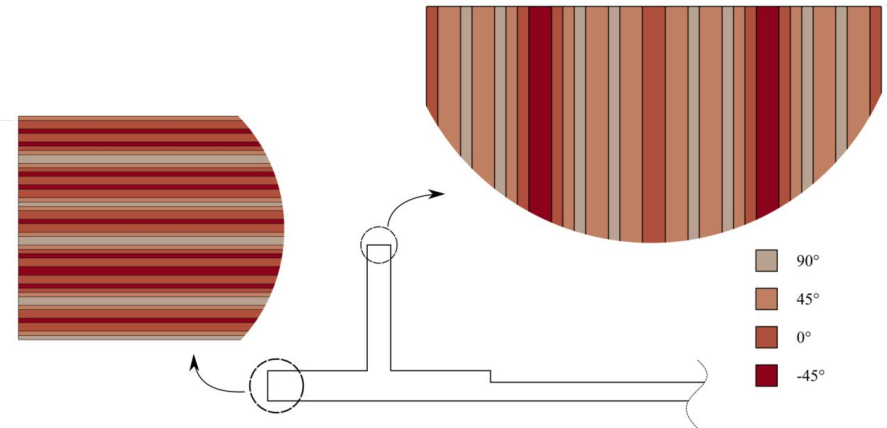
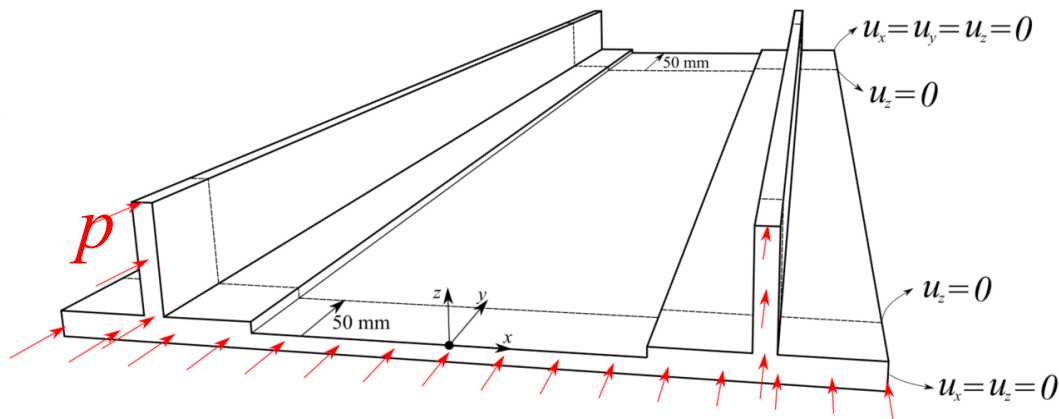
- Post-buckling (like) of cantilever composite beam



E. Carrera, A. Pagani, R. Augello, “Effect of large displacements on the linearized vibration of composite beams”, International Journal of Non-Linear Mechanics, 2020.

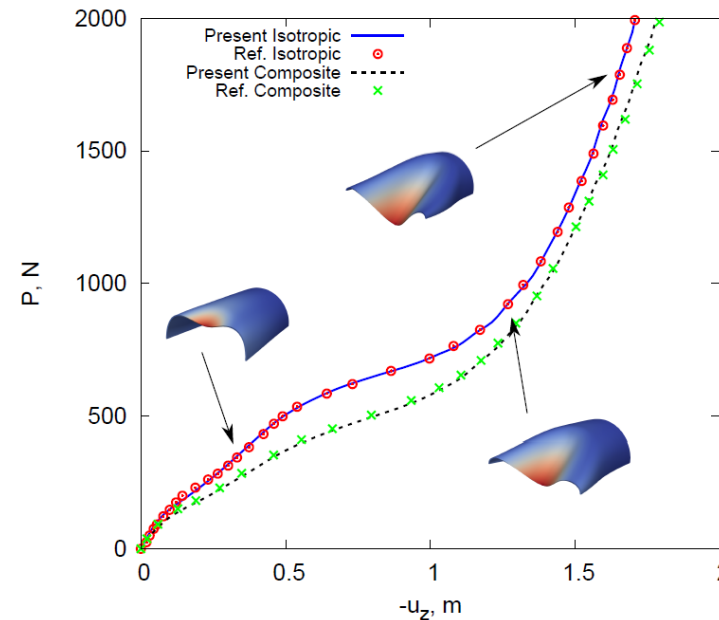
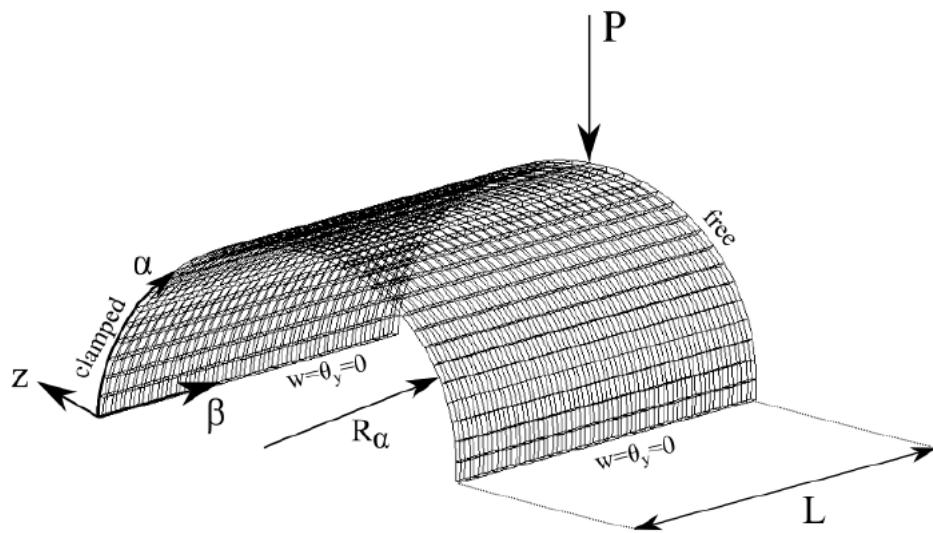
Numerical results – modal analysis - 1D model

- Reinforced panel

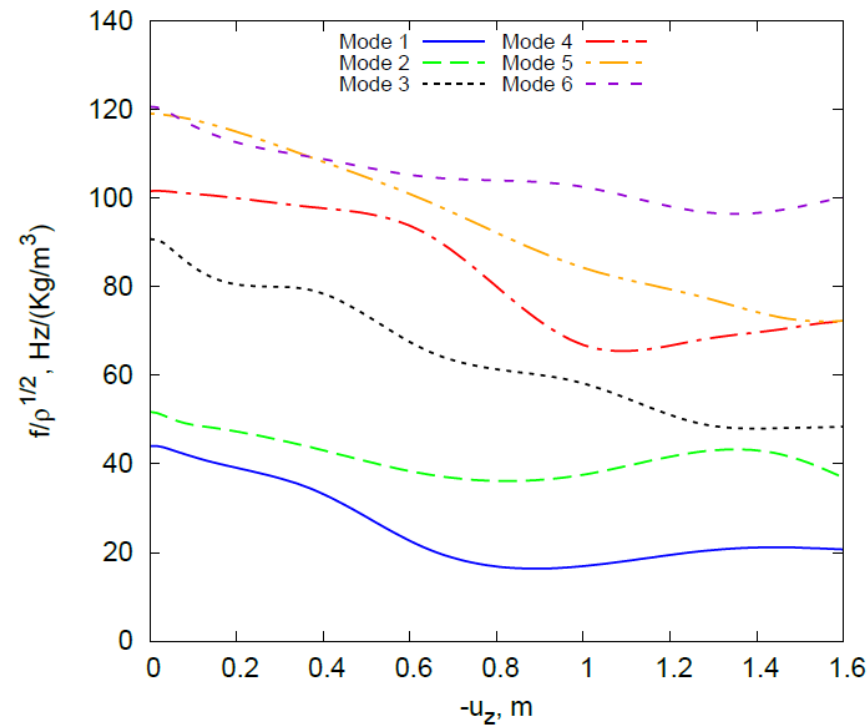
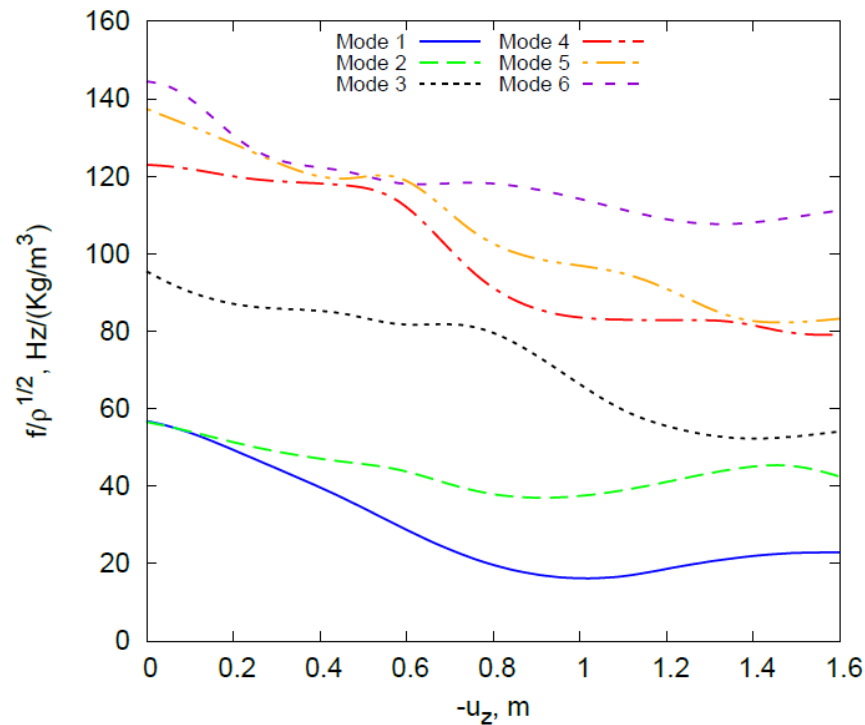


Numerical results – modal analysis - 2D shell model

- Pinched isotropic and composite cylinder

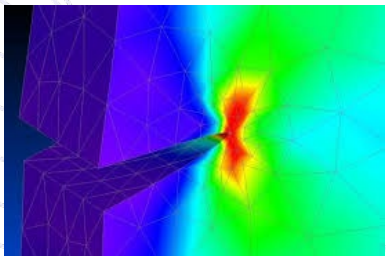


E. Carrera, A. Pagani, R. Azzara, R. Augello, "Vibration of metallic and composite shells in geometrical nonlinear equilibrium states", Thin-Walled Structures, 2020.

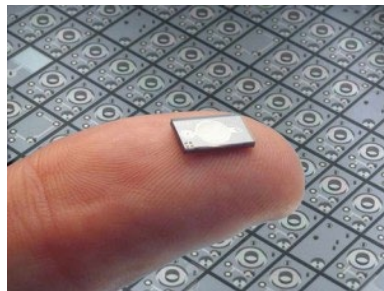


- In engineering and scientific applications, the **classical continuum** mechanics represents the most adopted tool to analyze structural problems. The interaction between adjacent points occur only by means of translational forces.
- However, in **many cases**, it may no longer represent an appropriate and reliable mathematical model to describe the physical phenomena that happen within the structure.

Large stress gradients in the proximity of holes



Size structure comparable to the microstructural scale



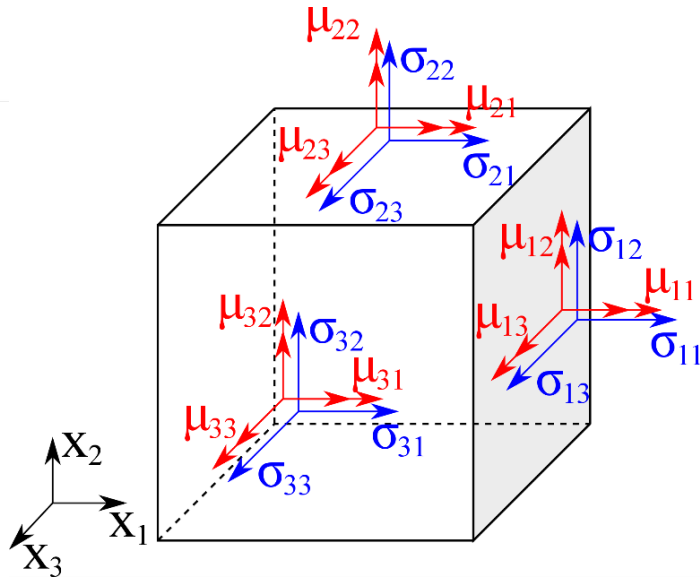
Unsymmetric stress and strain components

$$\boldsymbol{\sigma} = \begin{bmatrix} \sigma_{11} & \sigma_{21} & \sigma_{31} \\ \sigma_{12} & \sigma_{22} & \sigma_{32} \\ \sigma_{13} & \sigma_{23} & \sigma_{33} \end{bmatrix}$$

- Continuum mechanics classical elasticity
- Nonlocal elasticity (continuum and discrete)

Micropolar Elasticity

Formulation



$$\text{Force stress} \quad \sigma = \begin{bmatrix} \sigma_{11} & \sigma_{21} & \sigma_{31} \\ \sigma_{12} & \sigma_{22} & \sigma_{32} \\ \sigma_{13} & \sigma_{23} & \sigma_{33} \end{bmatrix} \quad \text{Strain} \quad \epsilon = \begin{bmatrix} \epsilon_{11} & \epsilon_{21} & \epsilon_{31} \\ \epsilon_{12} & \epsilon_{22} & \epsilon_{32} \\ \epsilon_{13} & \epsilon_{23} & \epsilon_{33} \end{bmatrix}$$

$$\text{Couple stress} \quad \mu = \begin{bmatrix} \mu_{11} & \mu_{21} & \mu_{31} \\ \mu_{12} & \mu_{22} & \mu_{32} \\ \mu_{13} & \mu_{23} & \mu_{33} \end{bmatrix} \quad \text{Twist} \quad \chi = \begin{bmatrix} \chi_{11} & \chi_{21} & \chi_{31} \\ \chi_{12} & \chi_{22} & \chi_{32} \\ \chi_{13} & \chi_{23} & \chi_{33} \end{bmatrix}$$

Strain-displacement relations:

- $\epsilon_{ij} = u_{i,j} + e_{ijk}\omega_k \quad i,j,k = 1,2,3$
- $\chi_{ij} = \omega_{i,j}$

Constitutive equations:

- $\sigma = \lambda(\text{tr}\epsilon)I + (\mu + \alpha)\epsilon + (\mu - \alpha)\epsilon^T$
- $\mu = \beta(\text{tr}\chi)I + (\gamma + \epsilon)\chi + (\gamma - \epsilon)\chi^T$

Unknowns

$$u_{(1,2,3)} = \{ \underbrace{u_1 \quad u_2 \quad u_3}_{\text{Displacement}} \quad \underbrace{\omega_1 \quad \omega_2 \quad \omega_3}_{\text{Micro-Rotation}} \}^T$$

Displacement

Micro-Rotation

Micropolar elastic constants



| Material | λ (MPa) | μ (MPa) | α (MPa) | β (N) | γ (N) | ε (N) |
|----------|-----------------|-------------|----------------|-------------|--------------|-------------------|
| HB | 4000 | 4000 | 63.49 | − 131.8 | 193.3 | 3046 |
| FPSF | 0.098 | 0.600 | 0.059 | − 6.685 | 9.126 | 50.87 |
| FDP | 416.0 | 104.0 | 4.333 | − 27.76 | 39.97 | 5.324 |
| FP | 762.6 | 103.9 | 4.333 | − 27.76 | 39.97 | 5.324 |
| FS | 2195 | 1033 | 114.7 | − 3.233 | 4,364 | 0.0534 |
| WF300 | 88.04 | 285.0 | 2.879 | 198.2 | 182.4 | 493.5 |
| WF110 | 550.0 | 75.00 | 0.758 | 40.97 | 20.28 | 16.47 |
| WF51 | 11.06 | 29.00 | 1.208 | 8.677 | 8.456 | 26.63 |
| AEC | 7590 | 1897 | 7.450 | 2240 | 2445 | 185.0 |

HB - Human Bone

FPSF - Polystyrene Foam

FDP - Dense Polyurethane Foam

FP - Polyurethane Foam

FS - Syntactic Foam

WF300/110/51 - Polymethacrylimide

Foam of the corresponding grade

AEC - Aluminum–Epoxy Composite



E. Carrera, V.V. Zozulya,
“Closed-form solution for the
micropolar plates: Carrera
unified formulation (CUF)
approach”, Archive of Applied
Mechanics, 2020.



W.B. Anderson, R. Lakes, “Size
effects due to Cosserat elasticity
and surface damage in closed-
cell polymethacrylimide
foam”, J. Mater. Sci, 1994.



R.D. Gauthier, W.E. Jahsman,
“A quest for micropolar elastic
constants”, J. Appl. Mech,
1975.



R. Lakes, “Experimental micro
mechanics methods for
conventional and negative
Poisson’s ratio cellular solids as
Cosserat continua”, J. Eng.
Mater. Technol., 1991.

Unified formulation of Micropolar Elasticity



R. Augello, E. Carrera, A. Pagani, "Unified theory of structures based on micropolar elasticity", Meccanica, 2019.

$$\bullet \quad \sigma = \lambda(\text{tr}\epsilon)I + (\mu + \alpha)\epsilon + (\mu - \alpha)\epsilon^T \longrightarrow \sigma = C \epsilon$$

$$\bullet \quad \mu = \beta(\text{tr}\chi)I + (\gamma + \epsilon)\chi + (\gamma - \epsilon)\chi^T \longrightarrow \mu = A \chi$$

$$C = \begin{bmatrix} C_{11} & C_{12} & C_{13} & 0 & 0 & 0 & 0 & 0 & 0 \\ C_{12} & C_{22} & C_{23} & 0 & 0 & 0 & 0 & 0 & 0 \\ C_{13} & C_{23} & C_{33} & 0 & 0 & 0 & 0 & 0 & 0 \\ 0 & 0 & 0 & C_{44}^M & C_{44}^{MT} & 0 & 0 & 0 & 0 \\ 0 & 0 & 0 & C_{44}^{MT} & C_{44}^M & 0 & 0 & 0 & 0 \\ 0 & 0 & 0 & 0 & 0 & C_{55}^M & C_{55}^{MT} & 0 & 0 \\ 0 & 0 & 0 & 0 & 0 & C_{55}^{MT} & C_{55}^M & 0 & 0 \\ 0 & 0 & 0 & 0 & 0 & 0 & 0 & C_{66}^M & C_{66}^{MT} \\ 0 & 0 & 0 & 0 & 0 & 0 & 0 & C_{66}^{MT} & C_{66}^M \end{bmatrix}$$

$$A = \begin{bmatrix} A_{11} & A_{12} & A_{13} & 0 & 0 & 0 & 0 & 0 & 0 \\ A_{12} & A_{22} & A_{23} & 0 & 0 & 0 & 0 & 0 & 0 \\ A_{13} & A_{23} & A_{33} & 0 & 0 & 0 & 0 & 0 & 0 \\ 0 & 0 & 0 & A_{44}^M & A_{44}^{MT} & 0 & 0 & 0 & 0 \\ 0 & 0 & 0 & A_{44}^{MT} & A_{44}^M & 0 & 0 & 0 & 0 \\ 0 & 0 & 0 & 0 & 0 & A_{55}^M & A_{55}^{MT} & 0 & 0 \\ 0 & 0 & 0 & 0 & 0 & A_{55}^{MT} & A_{55}^M & 0 & 0 \\ 0 & 0 & 0 & 0 & 0 & 0 & 0 & A_{66}^M & A_{66}^{MT} \\ 0 & 0 & 0 & 0 & 0 & 0 & 0 & A_{66}^{MT} & A_{66}^M \end{bmatrix}$$

$$C_{11} = C_{22} = C_{33} = \lambda + 2\mu,$$

$$C_{12} = C_{13} = C_{23} = \lambda,$$

$$C_{44}^M = C_{55}^M = C_{66}^M = \mu + \alpha,$$

$$C_{44}^{MT} = C_{55}^{MT} = C_{66}^{MT} = \mu - \alpha$$

$$A_{11} = A_{22} = A_{33} = \beta + 2\gamma,$$

$$A_{12} = A_{13} = A_{23} = \beta,$$

$$A_{44}^M = A_{55}^M = A_{66}^M = \gamma + \epsilon,$$

$$A_{44}^{MT} = A_{55}^{MT} = A_{66}^{MT} = \gamma - \epsilon$$

Unified formulation of Micropolar Elasticity

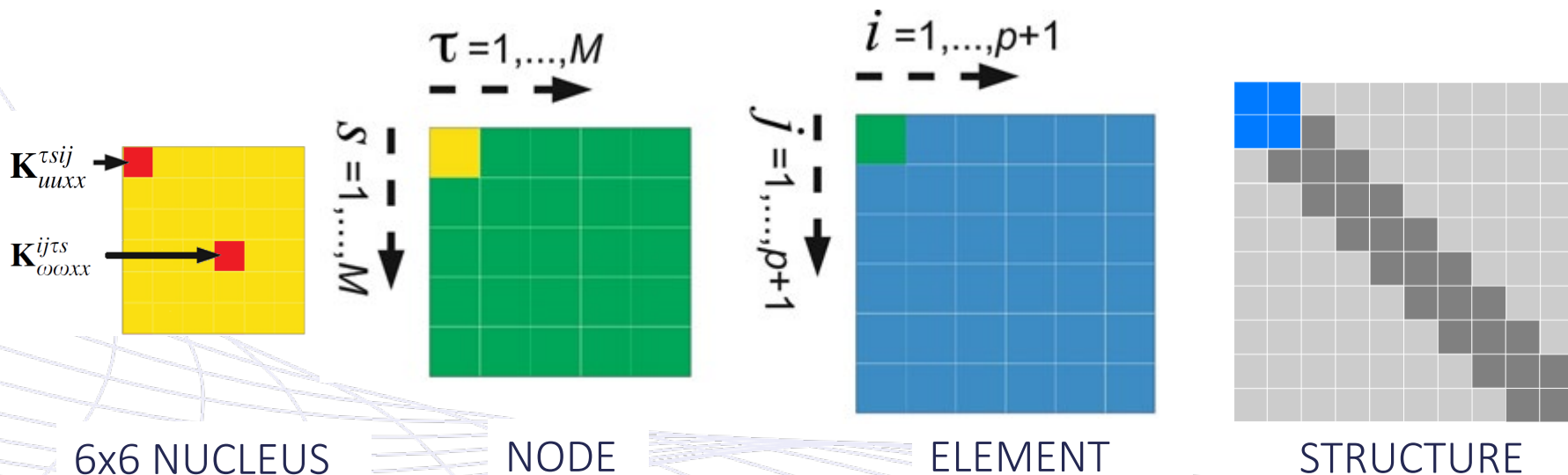
- Stiffness matrix



$$\begin{aligned}\delta L_{\text{int}} &= \int_V ((\delta \epsilon^T \sigma) + (\delta \chi^T \mu)) dV = \delta \mathbf{q}_{\tau i}^T \int ((\mathbf{B}_{m1}^{\tau i})^T \mathbf{C}(\mathbf{B}_{m1}^{sj}) + (\mathbf{B}_{m2}^{\tau i})^T \mathbf{A}(\mathbf{B}_{m2}^{sj})) dV \mathbf{q}_{sj} \\ &= \delta \mathbf{q}_{\tau i}^T \mathbf{K}^{ij\tau s} \mathbf{q}_{sj}\end{aligned}$$

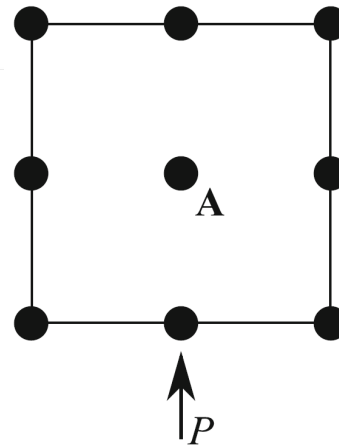
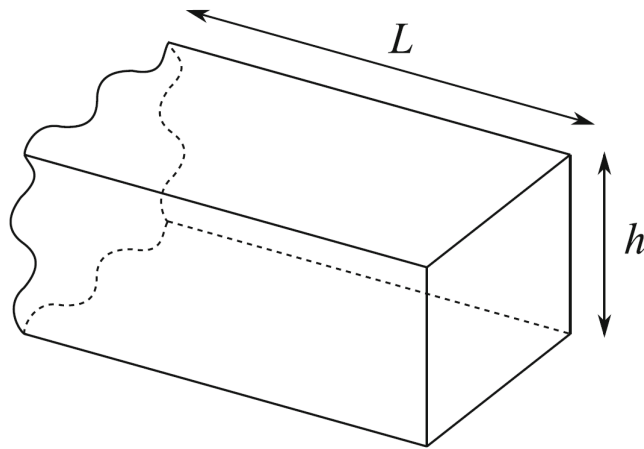
$$\begin{aligned}\mathbf{K}_{uuxx}^{\tau sij} &= C_{11} \int_{\Omega} F_{\tau,x} F_{s,x} d\Omega \int_L N_i N_j dL \\ &+ C_{55}^M \int_{\Omega} F_{\tau,z} F_{s,z} d\Omega \int_L N_i N_j dL \\ &+ C_{44}^M \int_{\Omega} F_{\tau} F_s d\Omega \int_L N_{i,y} N_{j,y} dL\end{aligned}$$

$$\begin{aligned}\mathbf{K}_{\omega\omega xx}^{ij\tau s} &= 2C_{66}^M \int_{\Omega} F_s F_t d\Omega \int_L N_i N_j dL \\ &- 2C_{66}^{MT} \int_{\Omega} F_s F_t d\Omega \int_L N_i N_j dL + \\ &A_{11} \int_{\Omega} F_{\tau,x} F_{s,x} d\Omega \int_L N_i N_j dL + A_{55} \int_{\Omega} F_{\tau,z} F_{s,z} d\Omega \\ &\times \int_L N_i N_j dL \\ &+ A_{44} \int_{\Omega} F_{\tau} F_s d\Omega \int_L N_{i,y} N_{j,y} dL\end{aligned}$$



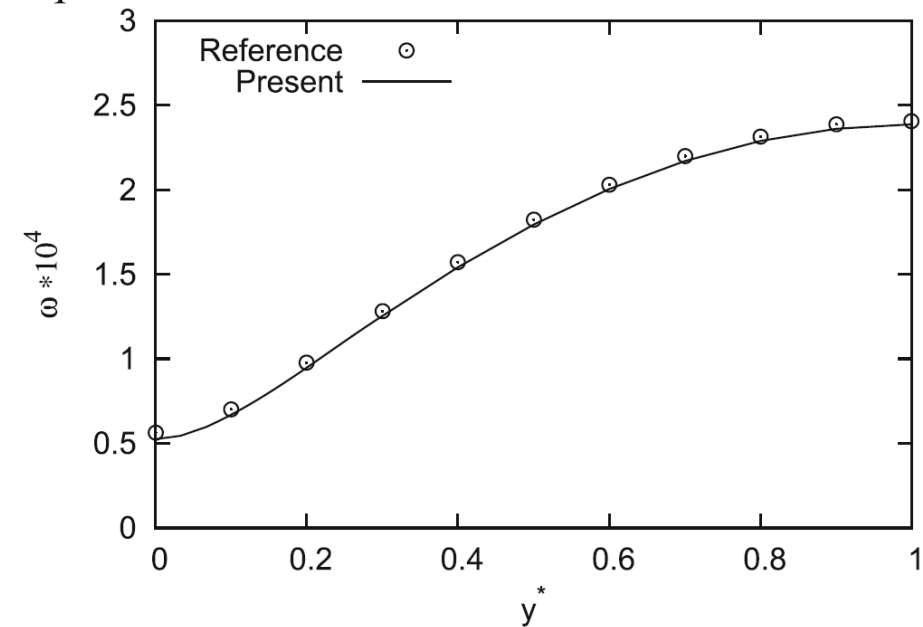
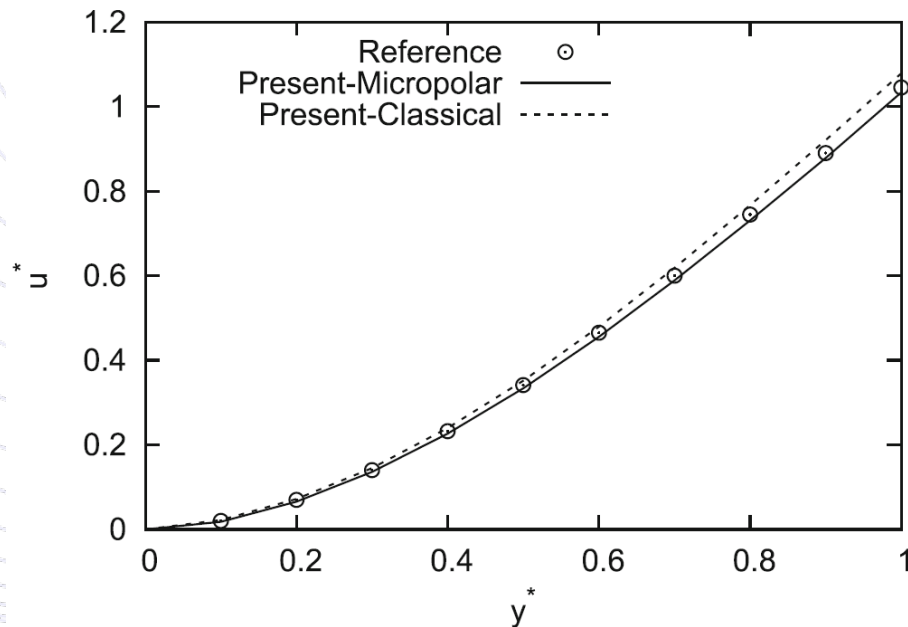
Numerical results – 1D model

- Assessment



$$\frac{\alpha}{E} = 10^{-2} \quad \frac{\gamma}{E} = \frac{\varepsilon}{E} = 2.5 * 10^{-4}$$

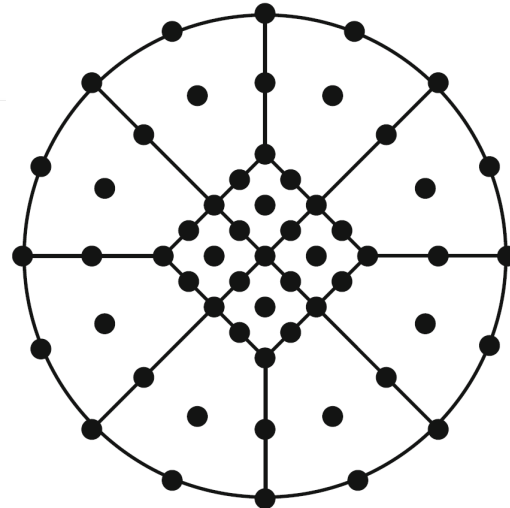
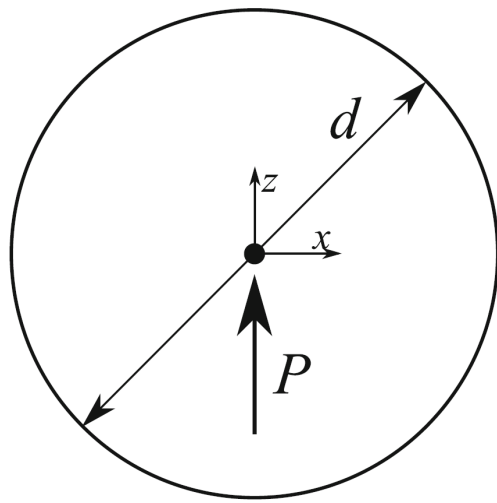
$$\frac{P}{EA} = 5 * 10^{-6} \quad \frac{L}{\sqrt{\frac{I}{A}}} = 10$$



S. Hassanpour, G.R. Heppler, “*Micropolar elasticity theory: a survey of linear isotropic equations, representative notations, and experimental investigations*”, Math. Mech. Solids, 2017.

Numerical results – 1D model

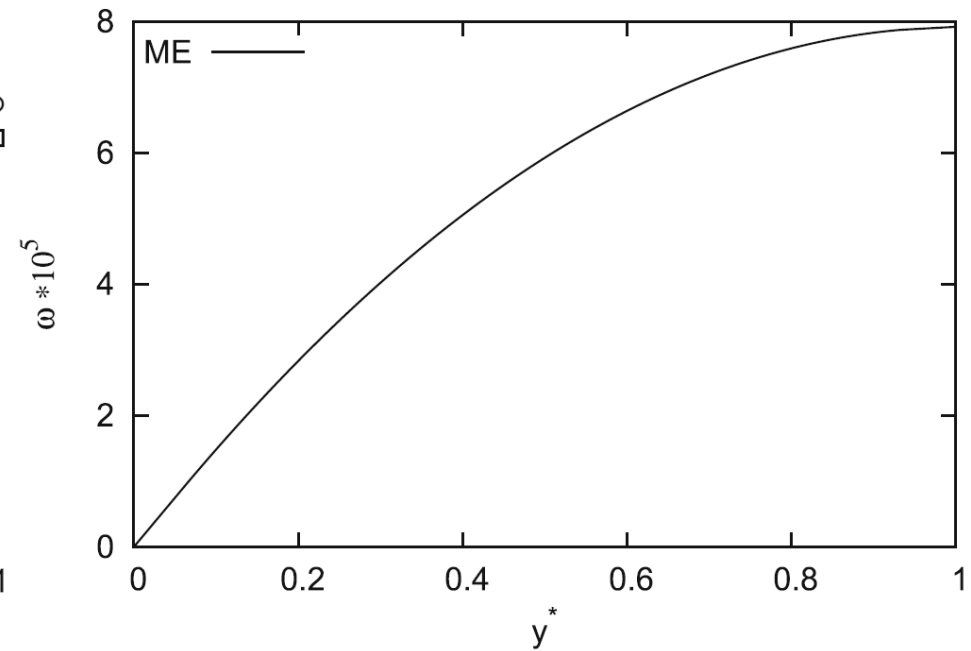
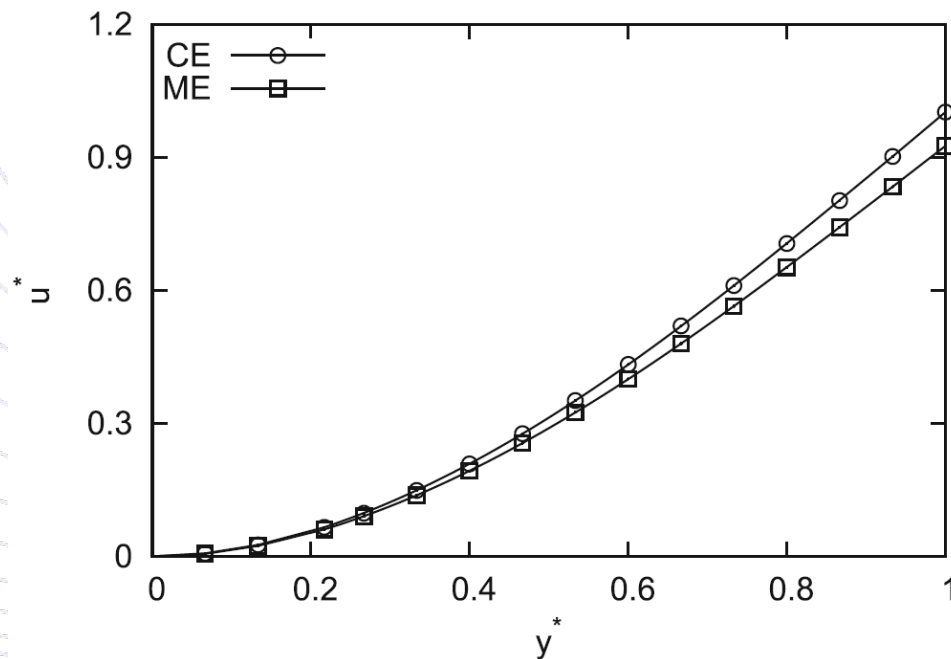
- Human bone



$$\begin{aligned}\lambda &= 4000 \text{ MPa} \\ \mu &= 4000 \text{ MPa} \\ \alpha &= 63.49 \text{ MPa} \\ \beta &= -131.8 \text{ N} \\ \gamma &= 193.3 \\ \varepsilon &= 3046 \text{ N}\end{aligned}$$



R. Lakes,
“Experimental
methods for study
of Cosserat
elastic solids and
other generalized
continua”, J.
(eds.)
Continuum
Models for
Materials with
Micro-structure,
1995.

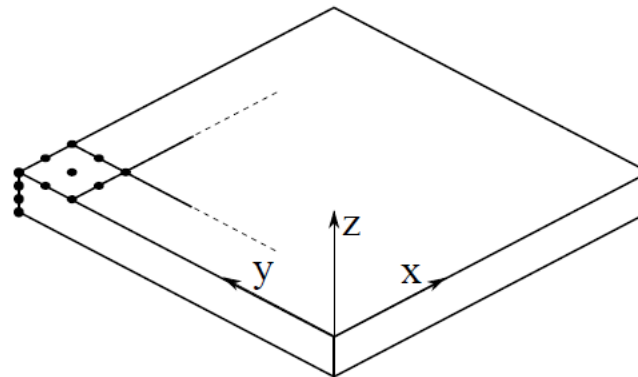
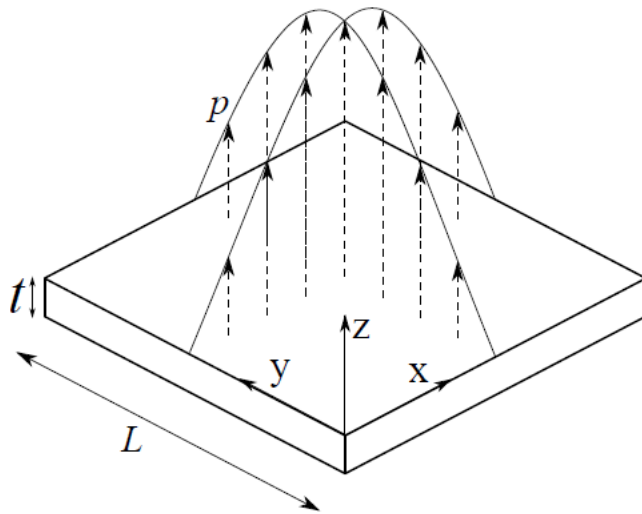


Numerical results – 2D plate model

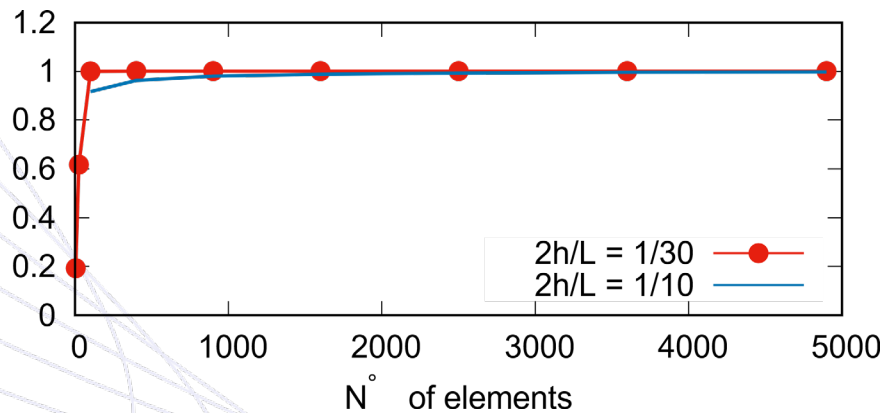
- Assessment on Polyurethane Foam plate



$$p(x, y) = p_0 \sin\left(\frac{\pi x}{L}\right) \sin\left(\frac{\pi y}{L}\right)$$



| Parameters | Values |
|------------|--------|
| λ | 762.6 |
| μ | 103.9 |
| E | 299.2 |
| ν | 0.44 |
| α | 4.333 |
| β | -27.76 |
| γ | 39.97 |
| ϵ | 5.324 |



| Mesh | Elements | $t/L = 1/10$ | | $t/L = 1/30$ | |
|-------|----------|--------------|---|--------------|---|
| | | u_z | $\frac{(u_z \text{ Ref.} - u_z)}{u_z \text{ Ref.}}$ | u_z | $\frac{(u_z \text{ Ref.} - u_z)}{u_z \text{ Ref.}}$ |
| 2x2 | 4 | | | 0.1304 | 80.71% |
| 5x5 | 25 | | | 0.4174 | 38.25% |
| 10x10 | 100 | 0.08053 | 8.26% | 0.6755 | 0.07% |
| 20x20 | 400 | 0.08454 | 3.69% | 0.6765 | -0.07% |
| 30x30 | 900 | 0.08597 | 2.06% | 0.6765 | -0.08% |
| 40x40 | 1600 | 0.08668 | 1.25% | 0.6765 | -0.09% |
| 50x50 | 2500 | 0.08709 | 0.79% | 0.6766 | -0.09% |
| 60x60 | 3600 | 0.08735 | 0.49% | | |
| 70x70 | 4900 | 0.08753 | 0.29% | | |

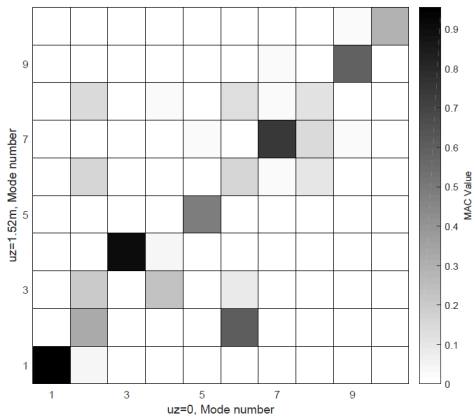


E. Carrera, V.V. Zozulya, "Closed-form solution for the micropolar plates: Carrera unified formulation (CUF) approach", Archive of Applied Mechanics, 2020.

Conclusions

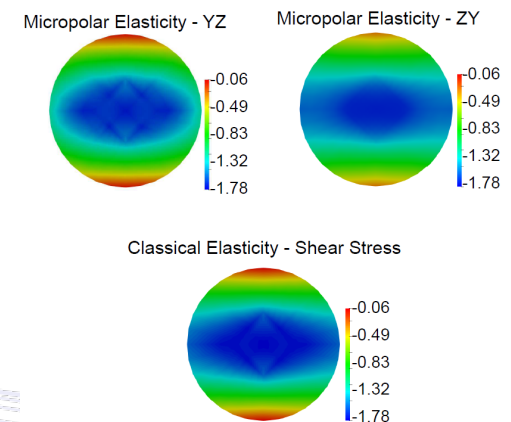
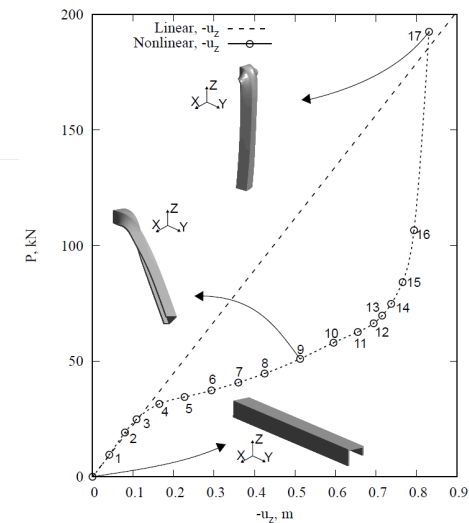


- In the recent past, **CUF** has been demonstrated to provide an efficient formulation for the development of refined kinematics beam models which can deal with higher-order phenomena. The nonlinear governing equations, along with the related finite element approximation, have been formulated using the principle of virtual work.



- The results show how modal shapes (and, subsequently, the associated natural frequencies) change when the structure is subjected to large displacement and rotation.

- CUF** has been demonstrated to provide an efficient formulation for the development of a unified formulation of Micropolar Elasticity, by comparing results with those from literature.



Publications

- Journal articles (1)



E. Carrera, A. Pagani, R. Azzara and R. Augello.
“Vibration of metallic and composite shells in geometrical nonlinear equilibrium states”,
Thin-Walled Structures, 2020.



A. Pagani, R. Azzara, R. Augello, E. Carrera and B. Wu.
“Accurate through-the-thickness stress distributions in thin-walled metallic structures subjected to large displacements and large rotations”,
Vietnam Journal of Mechanics, 2020.



E. Carrera, A. Pagani and R. Augello.
“Evaluation of geometrically nonlinear effects due to large cross-sectional deformations of compact and shell-like structures”,
Mechanics of Advanced Materials and Structures, 2020.



M.D. Demirbas, X. Xu, E. Carrera, H. Yang and R. Augello.
“Evaluation of stress distributions in the geometrical nonlinear regime of functionally graded structures”,
Composite Structures, 2020.



E. Carrera, A. Pagani and R. Augello.
“Effect of large displacements on the linearized vibration of composite beams”,
International Journal of Non-Linear Mechanic, 2020.



E. Carrera, A. Pagani, R. Augello and B. Wu.
“Popular benchmarks of nonlinear shell analysis solved by 1D and 2D CUF-based finite elements”,
Mechanics of Advanced Materials and Structures, 2020.



A. Pagani, R. Azzara, R. Augello and E. Carrera.
“Multibody simulation and descent control of a space lander”,
Advances in aircraft and spacecraft science 2020.



X. Xu, R. Augello and H. Yang.
“The generation and validation of a CUF-based FEA model with laser-based experiments”,
Mechanics of Advanced Materials and Structures, 2019.



X. Xu, H. Yang, R. Augello and E. Carrera.
“Optimized free-form surface modeling of point clouds from laser-based measurement”,
Mechanics of Advanced Materials and Structures, 2019.



R. Augello, E. Carrera, A. Pagani
“Unified theory of structures based on micropolar elasticity”,
Meccanica, 2019.

Publications

- Journal articles (2)



A. Pagani, E. Carrera and R. Augello.

“Evaluation of various geometrical nonlinearities in the response of beams and shells”,
AIAA Journal, 2019.



A. Pagani, R. Augello and E. Carrera.

“Large deflection and post-buckling of thin-walled structures by finite elements with node-dependent kinematics”,
Acta Mechanica, 2021.



A. Pagani, R. Augello, G. Governale and A. Viglietti.

“Drop Test Simulations of Composite Leaf Spring Landing Gears”,
Aerotecnica Missili & Spazio, 2018.



E. Carrera , A. Pagani and R. Augello.

“On the role of large cross-sectional deformations in the nonlinear analysis of composite thin-walled structures”,
Archive of Applied Mechanics, 2021.



A. Pagani, R. Augello and E. Carrera.

“Frequency and mode change in the large deflection and post-buckling of compact and thin-walled beams”,
Journal of Sound and Vibration, 2018.



A. Pagani, R. Azzara, R. Augello and E. Carrera.

“Stress states in highly flexible thin-walled composite structures by unified shell model”,
Submitted.



A. Stio, P. Spinolo, E. Carrera and R. Augello.

“Analysis of landing mission phases for robotic exploration on phobos mar's moon”,
Advances in Aircraft and Spacecraft Science, 2017.



E. Carrera, A. Pagani, D. Giusa and R. Augello.

“Nonlinear analysis of thin-walled beams with highly deformable sections”,
International Journal of Non-Linear Mechanics, 2021.



A. Pagani, E. Carrera and R. Augello.

*“Vibrations of structures subjected to pre-stress states”,
In Italian Association of Aeronautics and Astronautics -
XXIV International Conference (AIDAA 2017), Palermo -
Enna, Italy, 18-22 September, 2017.*



A. Pagani, E. Carrera and R. Augello.

*“Mode change in nonlinear dynamics of laminated
structures”,
In 20th International Conference on Composite Structures
(ICCS20), Paris, France, September 4-7, 2017.*



R. Augello, E. Carrera and A. Pagani.

*“Unified theory of structures based on micropolar
elasticity”,
In 1st International Conference on Mechanics of
Advanced Materials and Structures (ICMAMS), Torino,
Italy, 17-20 June, 2018.*



A. Pagani, R. Augello, and E. Carrera.

*“Effects of geometric nonlinearities on refined structural
models of laminated beams”,
In 10th European Solid Mechanics Conference, Bologna,
Italy, July 2-6, 2018.*



E. Carrera, A. Pagani and R. Augello.

*“Virtual vibration correlation technique (VCT) for nonlinear
buckling analysis of metallic and composite structures”,
In ASME's International Mechanical Engineering Congress
and Exposition (IMECE), Pittsburgh, PA, USA, 9-15
November, 2018.*



E. Carrera, A. Pagani and R. Augello.

*“Evaluation of in-plane and out-of-plane stresses in composite
structures subjected to large displacements/rotations”,
In ASME's International Mechanical Engineering Congress and
Exposition (IMECE), Pittsburgh, PA, USA, 9-15 November, 2018.*



**R. Augello, E. Carrera, W. Chen, M. Filippi, A. Pagani
and B. Wu.**

*“Effect of in-plane loadings on the free vibration of plates
in nonlinear regime”,
In First International Nonlinear Dynamics Conference
(NODYCON 2019), Rome, Italy, February 17-20, 2019.*



R. Augello, A. Pagani and E. Carrera.

*“Micropolar elasticity by unified theory”,
The 15th Jiangsu – Hong Kong Forum on Mechanics
and Its Application tenutosi a Hong Kong nel 13 Aprile
2019.*



E. Carrera, R. Augello and A. Pagani.

Preliminary technical report: Drop-tests of the main landing gear of Leonardo F48 UAV, 2017.



E. Carrera, R. Augello, A. Pagani and A. Viglietti.

Preliminary technical report: Finite element structural analyses of the nose landing gear of Leonardo F48 UAV, 2017.



E. Carrera, R. Augello, A. Pagani and A. Viglietti.

Preliminary technical report: Finite element structural analyses of the main landing gear of Leonardo F48 UAV, 2017.



E. Carrera, R. Augello and A. Pagani.

Preliminary technical report: Multi-body analysis of the nose landing gear of Leonardo F48 UAV, 2017.



E. Carrera, R. Augello and A. Pagani.

Preliminary technical report: Drop-tests of the nose landing gear of Leonardo F48 UAV, 2017.



E. Carrera, R. Augello and A. Pagani.

Preliminary technical report: Multi-body analysis of the main landing gear of Leonardo F48 UAV, 2017.



E. Carrera, R. Augello and A. Pagani.

Technical report: Multi-body analysis of the main landing gear of Leonardo F48 UAV, 2018.



E. Carrera, R. Augello and A. Pagani.

Technical report: Drop-tests of the nose landing gear of Leonardo F48 UAV, 2018.



E. Carrera, R. Augello and A. Pagani.

Technical report: Drop-tests of the main landing gear of Leonardo F48 UAV, 2018.



E. Carrera, R. Augello and A. Pagani.

Technical report: Drop-tests of the main landing gear of Leonardo F48 UAV, 2018.



E. Carrera, R. Augello, A. Pagani and A. Viglietti.

Technical report: Finite element structural analyses of the main landing gear of Leonardo F48 UAV, 2018.



E. Carrera, R. Augello, A. Pagani and A. Viglietti.

Technical report: Finite element structural analyses of the nose landing gear of Leonardo F48 UAV, 2018.